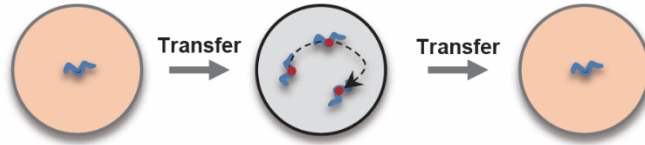


Each day of adulthood

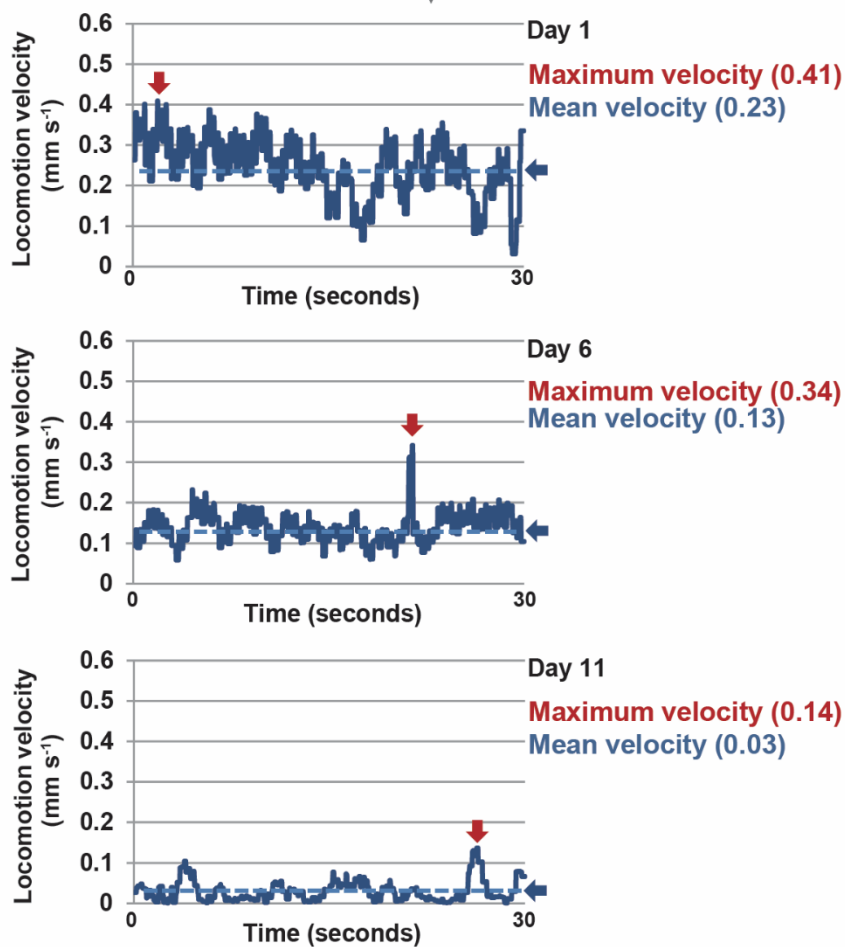
Growth plate (NGM plate with *E. coli* lawn) Physical assay plate (NGM without *E. coli* lawn) Growth plate (NGM plate with *E. coli* lawn)



Video recording for 30 seconds
(30 frames per second)

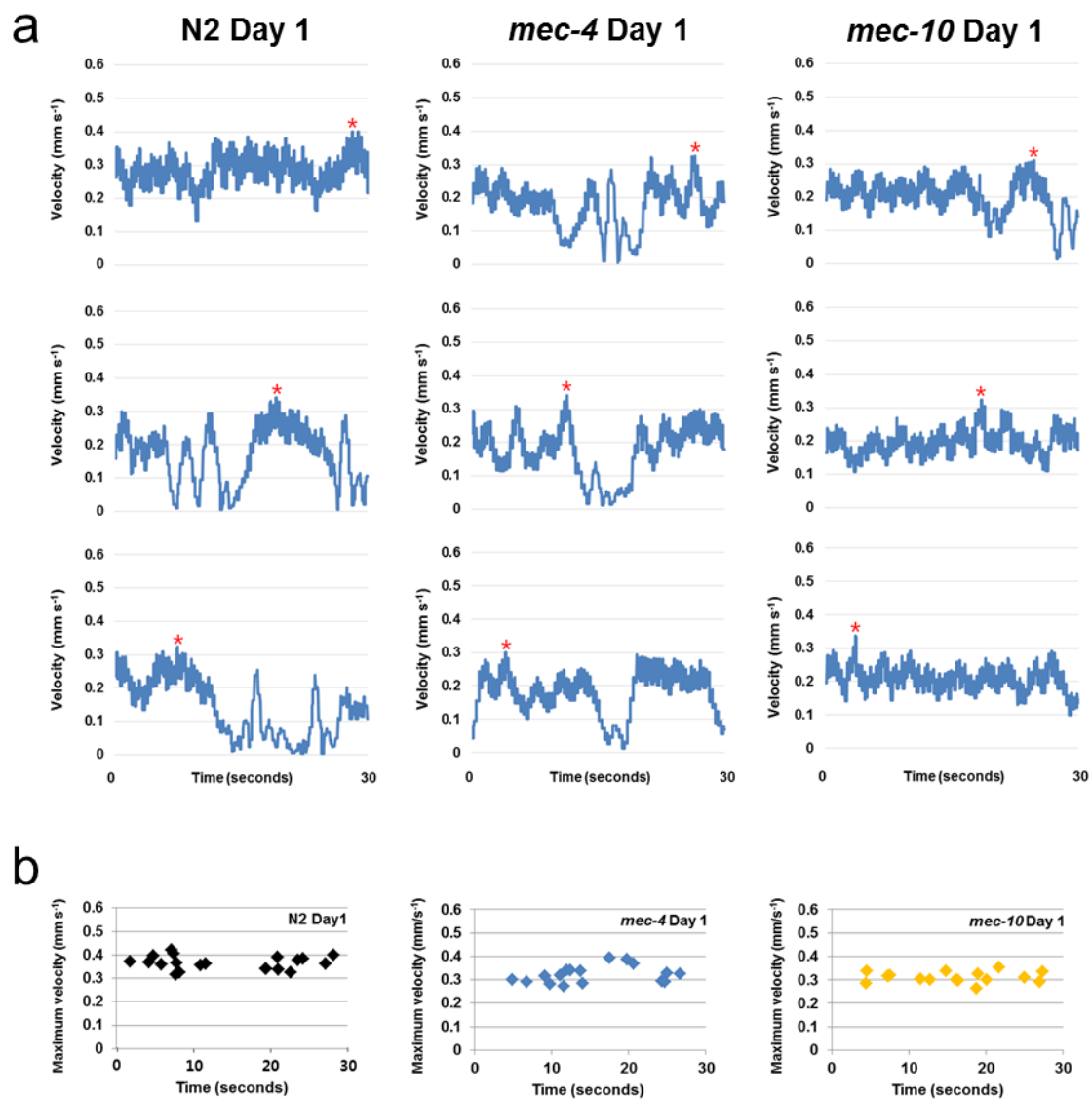
Data analysis

The distance (mm) between displaced centroids per second was analyzed by ImageJ and wrMTrck

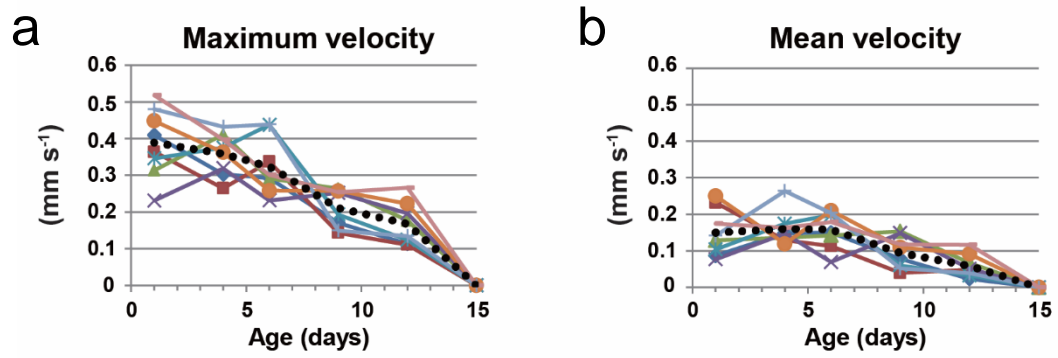


Supplementary Figure 1: The assay scheme for measuring the age-associated decline of short physical performances in *C. elegans*.

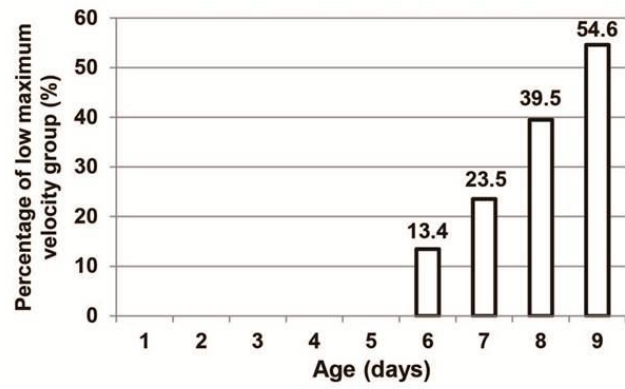
Worms were grown on a growth plate covered with a bacterial lawn. When measuring the physical performance, the worms were transferred to a 'physical assay plate' with no bacterial lawn and their movement was recorded for 30 seconds. The red dots indicate the centroids used to follow the movement of the worms. ImageJ and wrMTrck were used to calculate the locomotion velocity, which was expressed as mm s^{-1} [distance (mm) between centroid displacements per second]. The velocity profiles of a single worm at the three different ages (Day 1, 6, and 11 of adulthood) are shown at the bottom. The MV and mean velocity at the three different ages are noted.



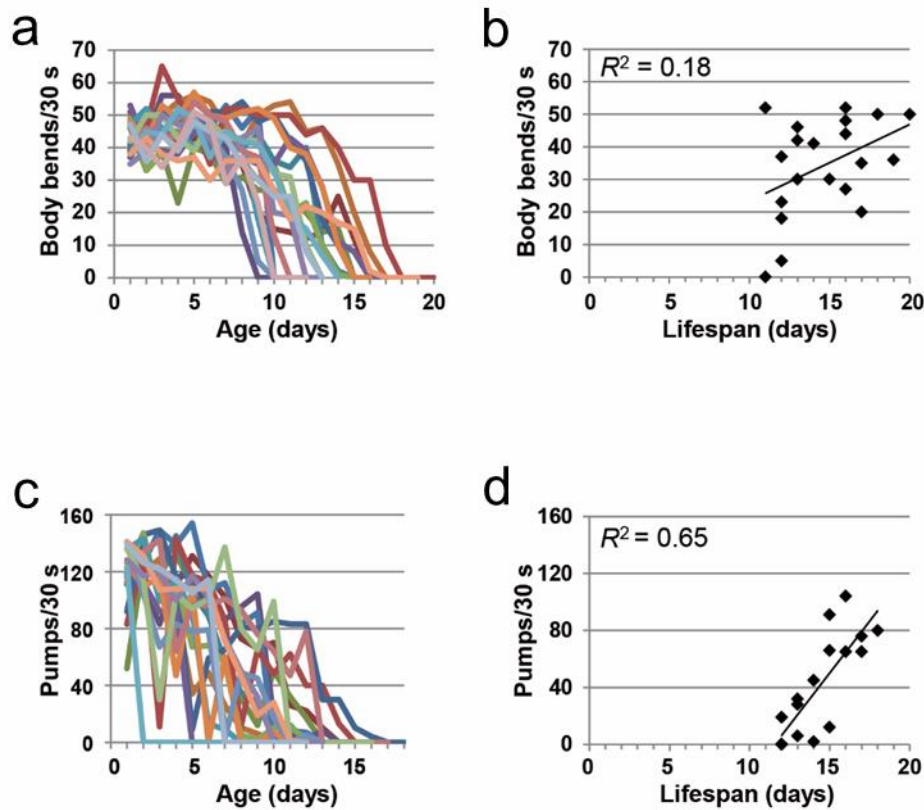
Supplementary Figure 2: Harsh-touch mutants do not behave differently from wild-type in the maximum velocity (MV) assay. (a) Mechanosensory mutants (*mec-4* and *mec-10*) show a velocity pattern similar to that of wild type in the MV assay. Red asterisk represents maximum velocity. **(b)** Maximum velocity appeared randomly on the 30 seconds interval of the MV assay in both wild type and mechanosensory mutants.



Supplementary Figure 3: Age-dependent changes of maximum (a) and mean (b) velocity of individual worms. Black dots represent the average value at each age ($n = 8$).



Supplementary Figure 4: Age-associated increase of percentage of low MV group ($n = 119$).



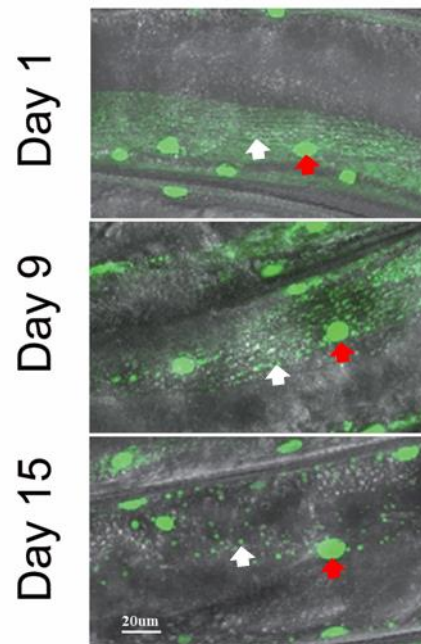
Supplementary Figure 5: Age-dependent changes in the thrashing and pharyngeal pumping.

(a) Age-associated change of thrashing. Thrashing of each worm is noted as body bends/30 s. **(b)** Correlation between thrashing and lifespan of individual worms.

Thrashing of individual worms was measured at Day 9 of adulthood and their lifespans were measured thereafter. R^2 , coefficient of determination. $n = 20$. **(c)** Age-associated change of pharyngeal pumping rate.

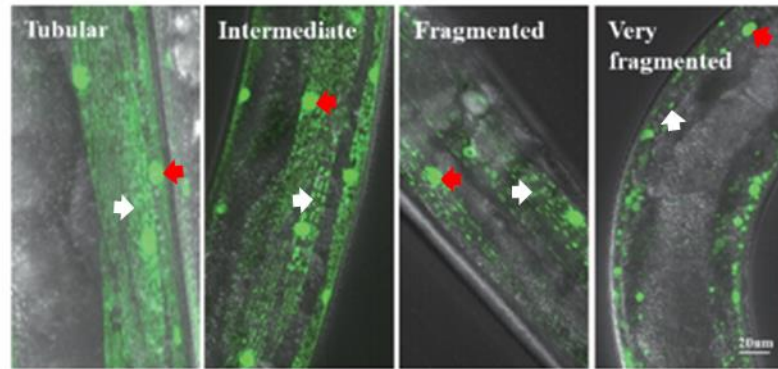
(d) Correlation between pharyngeal pumping and lifespan of individual worms. The pumping rates of individual worms were measured at Day 9 of adulthood and their lifespans were measured thereafter. R^2 , coefficient of determination. $n = 19$.

Note that, although the pharyngeal pumping rates showed a coefficient of determination value of 0.65, they showed highly irregular patterns along aging and thus do not serve as a good age-associated indicator.



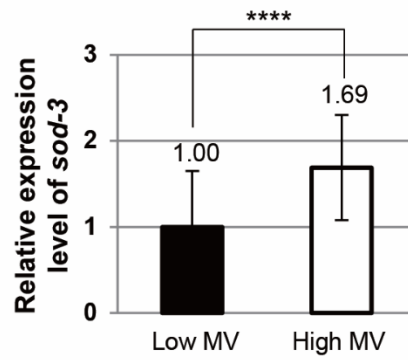
Supplementary Figure 6: Age-dependent changes of mitochondrial morphology in wild-type worms.

Top: mitochondria in the muscle cell of a worm at Day 1 of adulthood show tubular and intermediate morphology. Middle: fragmented mitochondria appear in a worm at Day 9 of adulthood. Bottom: mitochondria in a worm at Day 15 of adulthood are very fragmented with a few globular organelles. Colored green is the green fluorescence protein produced in mitochondria (white arrow) and nucleus (red arrow) in body wall muscles of PD4251 worms.



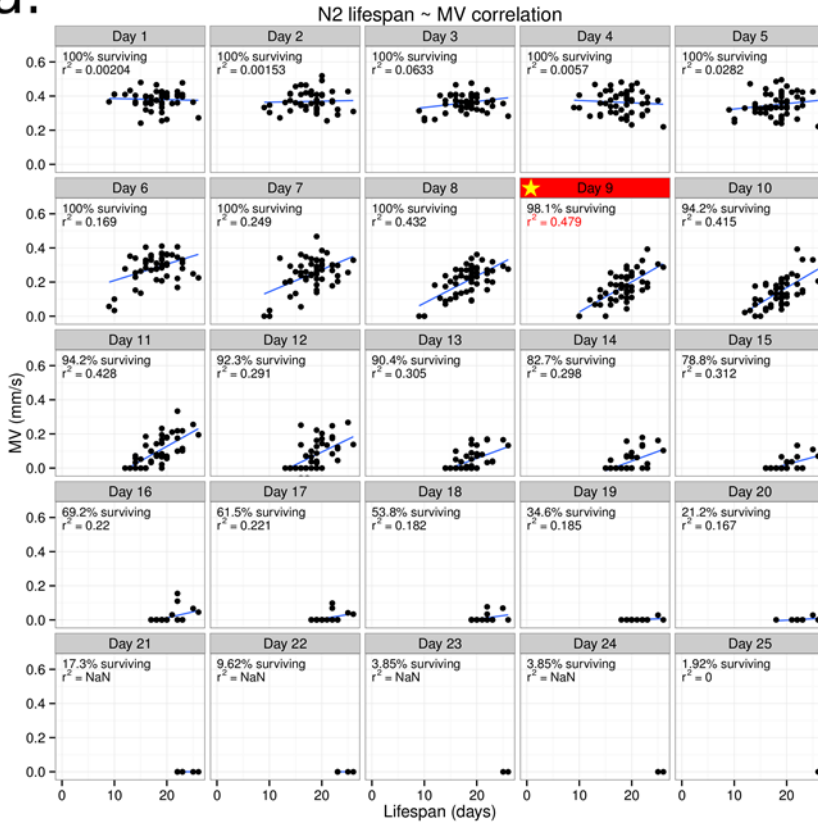
Score: 4 3 2 1

Supplementary Figure 7: Scoring of mitochondrial morphologies for mitochondrial integrity. To assay mitochondrial integrity, the scores of 1, 2, 3, and 4 were given to mitochondria with very fragmented, fragmented, intermediate, and tubular morphologies, respectively. Colored green is the green fluorescence protein produced in mitochondria (white arrow) and nucleus (red arrow) in body wall muscles of PD4251 worms.

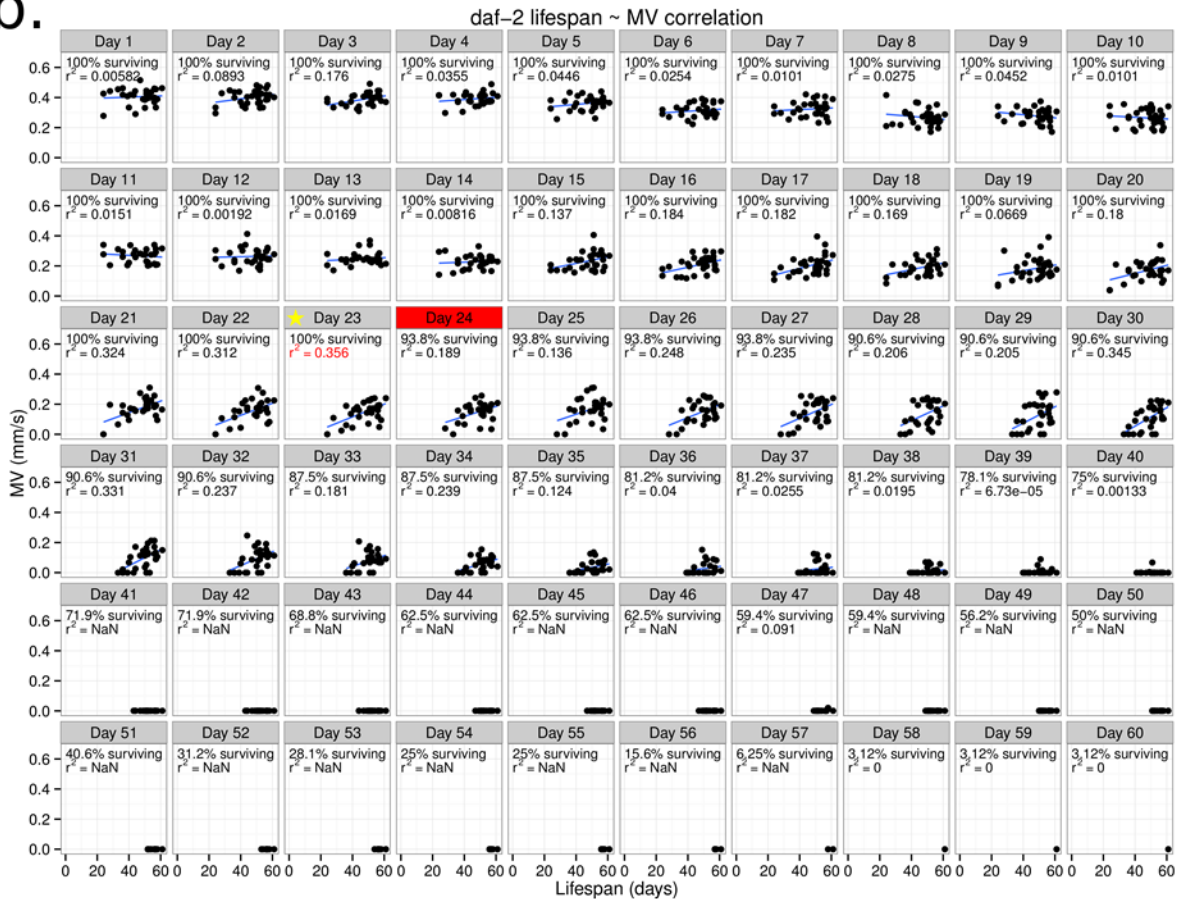


Supplementary Figure 8: Correlation of *sod-3* gene expression with MV in the low and high MV groups at Day 9 of adulthood. Significance was determined using a two-tailed, unpaired *t*-test. **** $P < 0.0001$. Error bars represent s.d.

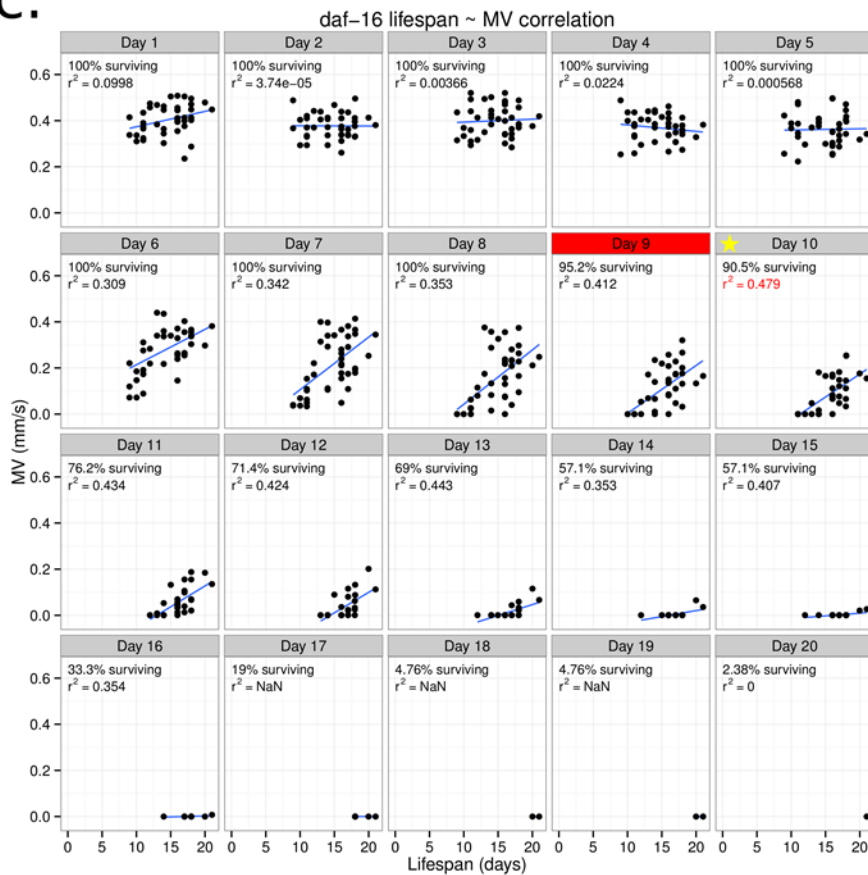
a.



b.



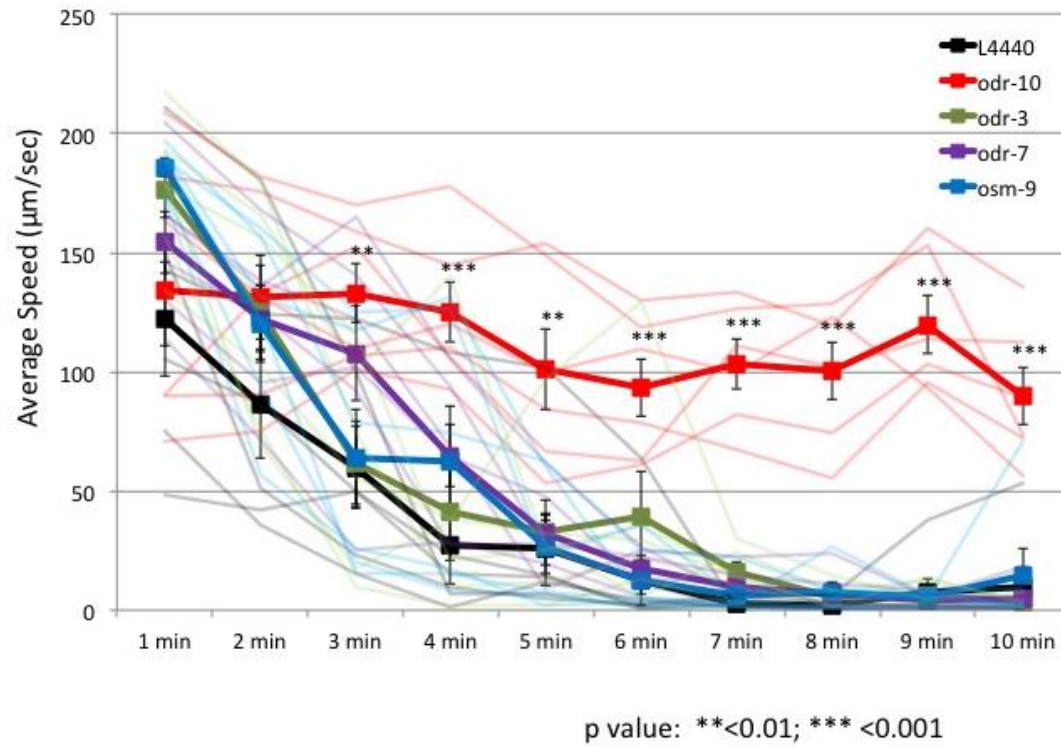
C.



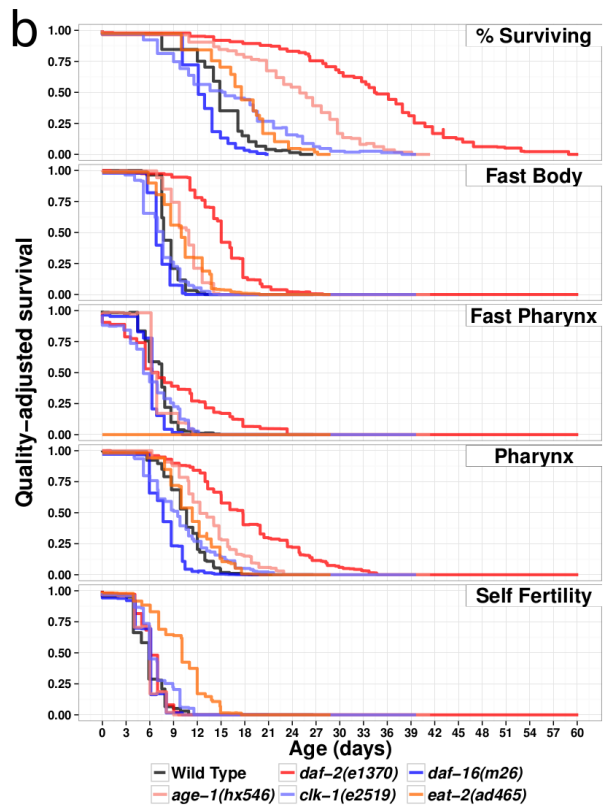
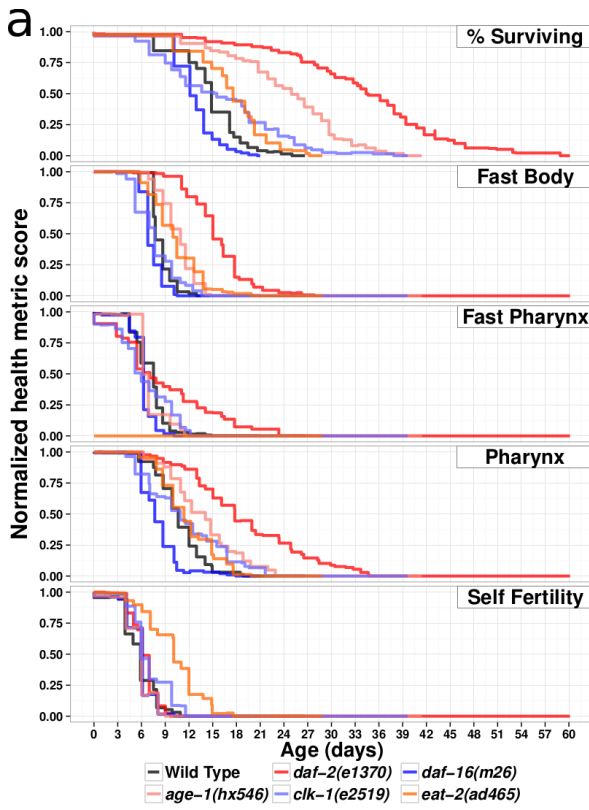
Supplementary Figure 9: Correlation between MV and lifespan for a cohort of worms tracked longitudinally through their lifespan.

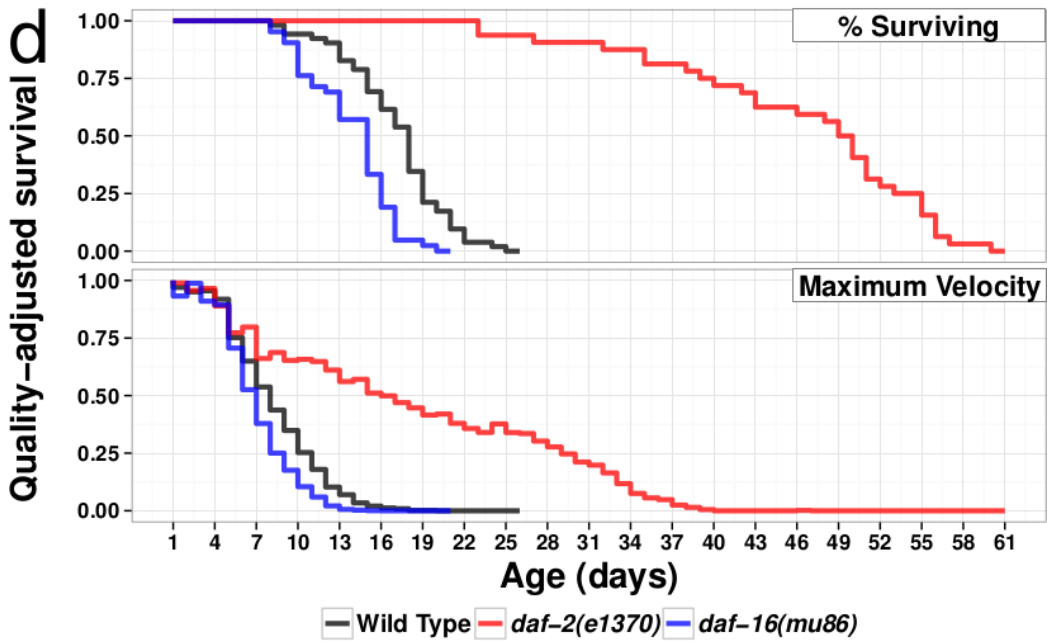
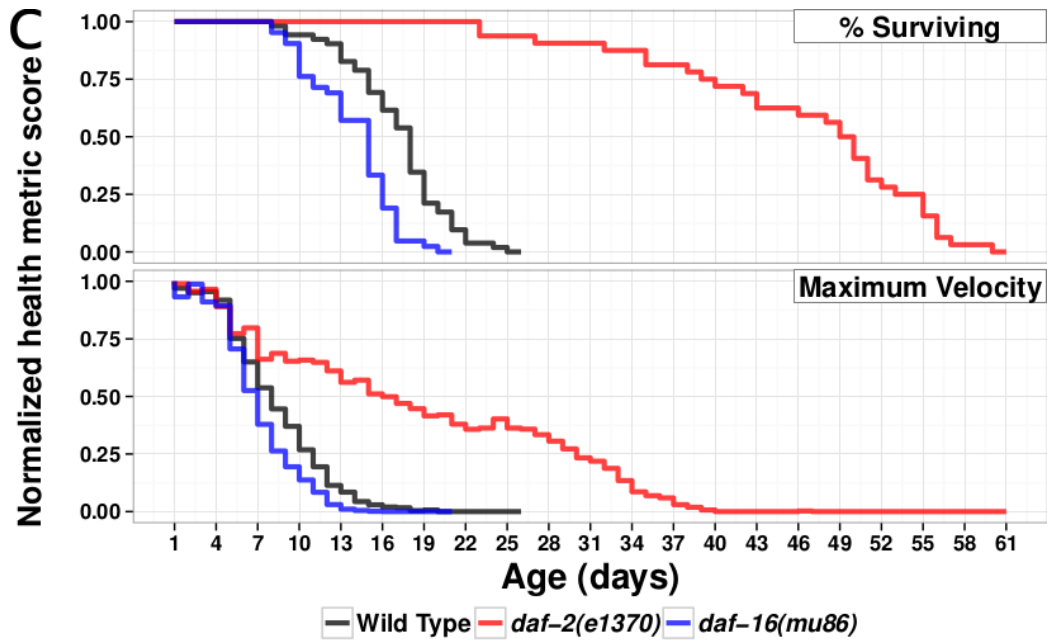
The day on which the first worm of the cohort dies is highlighted in red, and the day on which MV best correlates with lifespan is denoted with a star. In all cases tested, the best correlation between MV and lifespan occurs within a day of the first death of the cohort. **(a)** N2 worms tracked in Fig. 1a. The best correlation between MV and lifespan occurs on day 9, which is also when the first worm of the cohort dies. **(b)** *daf-2(e1370)* worms tracked in Fig. 2b. The best correlation between MV and lifespan occurs on day 23, the day before the first worm of the cohort dies. **(c)** *daf-16(mu86)* worms tracked in Fig. 2c. The best correlation occurs on day 10, the day after the first worm of the cohort dies.

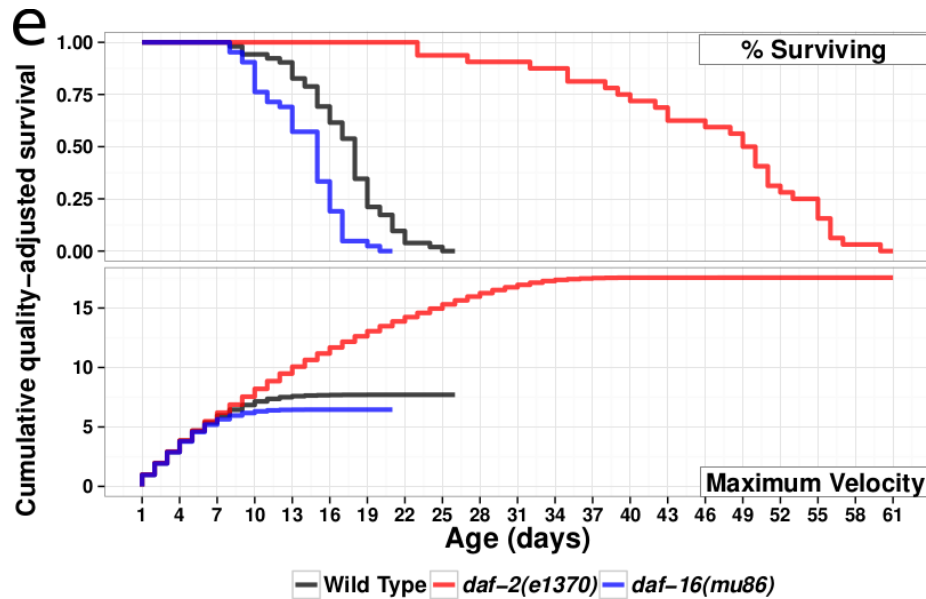
Day 1 *daf-2(e1370)* hermaphrodites



Supplementary Figure 10: On-bacteria motility assay. *daf-2(e1370)* worms after being raised on L4440 (control), *odr-3*, *odr-7*, or *osm-9* RNAi slow down soon after being placed onto bacteria, while *daf-2(e1370)* worms treated with *odr-10* RNAi (red) maintain a higher speed over the entire 10 min of the assay.







Supplementary Figure 11: Additional quality-adjusted health metrics

daf-2(e1370) mutants are healthier and have higher quality lives as measured in previous surveys of healthspan. (a) Quality-adjusted lifespan curves for the health categories, as scored by Huang et al.,¹ with categories separated by the health categories used in the study. (b) The Quality-adjusted lifespan curve is the survival rate multiplied by the health measurement, normalized to the maximum value attained by the wild type. From our own data on MV with age, we find *daf-2* mutants have higher quality life than wild type. (c), Quality-adjusted lifespan curves for MV as measured in this study. (d) Cumulative area under curve of the quality-adjusted MV lifespan, indicating higher total quality for *daf-2* mutants, and lower total quality for *daf-16(mu86)* mutants as compared to wild type. (e) Cumulative area under curve of the quality-adjusted MV.

Supplementary Reference

1. Huang C, Xiong CJ, Kornfeld K. Measurements of age-related changes of physiological processes that predict lifespan of *Caenorhabditis elegans*. *Proc Natl Acad Sci U S A* **101**, 8084-8089 (2004).